JOURNAL OF THE ROYAL SOCIETY Interface

CrossMark click for updates

J. R. Soc. Interface (2012) **9**, 2109–2119
doi:10.1098/rsif.2012.0006
Published online 18 April 2012

Acute inflammatory response to cobalt chromium orthopaedic wear debris in a rodent air-pouch model

Moeed Akbar[1], Alasdair R. Fraser[2], Gerard J. Graham[2], James M. Brewer[2] and M. Helen Grant[1,*]

[1]*Bioengineering Unit, University of Strathclyde, 106 Rottenrow, Wolfson Centre, Glasgow G4 0NW, UK*
[2]*Institute of Infection, Immunity and Inflammation, University of Glasgow, Sir Graham Davies Building, 120 University Place, Glasgow G12 8TA, UK*

This study used a rodent air-pouch model to assess the acute inflammatory response to cobalt–chromium (CoCr) alloy wear debris from a metal-on-metal hip resurfacing implant that may contribute to joint failure. Air-pouches were injected with either sterile phosphate-buffered saline, 1 μg lipopolysaccharide (LPS) or 2.5 mg CoCr wear debris. The *in situ* inflammatory response was monitored 4, 24, 48 and 72 h and 7 days later. A flow cytometric analysis of the inflammatory exudates showed that CoCr wear debris induced a different inflammatory pattern compared with LPS. LPS induced a strong early (4 h) neutrophil influx, with monocyte/macrophage influx peaking at 24 h, whereas CoCr wear debris initiated almost equal numbers of early monocyte/macrophage and neutrophil recruitment. Histological analyses also showed CoCr debris accumulated in the pouch wall and this was accompanied by vast cellular infiltration and fibrosis around the debris throughout the duration of the experiment. Assessment of inflammatory gene transcripts from air-pouch tissue showed that CoCr wear debris increased the expression of cytokines involved in promoting inflammation and fibrosis (IL-1β, TGF-β) and chemokines that promote the recruitment of neutrophils and monocytes/macrophages (CXCL2 and CCL2). The data suggest that inflammatory responses to CoCr debris induce a specific acute process in which the recruitment of monocytes/macrophages is key.

Keywords: inflammation; air-pouch model; orthopaedic implant; debris; leukocyte; cobalt–chromium alloy

1. INTRODUCTION

Metal-on-metal (MoM) hip resurfacing has become increasingly common in the management of osteoarthritis and represents 6–8% of all hip arthroplasties. Unfortunately, hip resurfacing also has one of the highest revision rates of all primary hip replacement procedures; in particular, certain MoM hip resurfacing prostheses show extremely high revision levels (greater than 10%) 5 years post surgery [1]. One of the hypothesized reasons for this failure is a peri-prosthetic soft tissue reaction to wear debris released from the implant, termed adverse reactions to metal debris (ARMD) [2]. Although the wear rate of articular surfaces with MoM prostheses is lower than with other more conventional bearings (i.e. metal-on-polyethylene), MoM implants tend to produce a broader size range of wear particles. These range from the nanometre scale, with the majority of particles between 15 and 25 nm, to aggregates of particles with diameters as large as 400 μm. It is estimated that up to 2.4×10^{14} metal particles are produced per year from a single MoM hip implant [3].

ARMD includes a range of clinical and histological effects. These include a rash, pain in the hip region and/or presence of a soft tissue mass (pseudotumour) surrounded by extensive necrosis and granuloma formation [4]. A specific characteristic of the tissues from patients affected by metal wear and metal ion release is aseptic lymphocytic vasculitis-associated lesion (ALVAL). ALVAL has been described as lymphocytic aggregates around the hip capsule and similar intense lymphocyte infiltrates have been reported around pseudotumours. It is postulated that ARMD is an inflammatory process in response to excessive particulate metal wear debris [4–6].

It is accepted that most biomaterials induce an acute inflammatory response following implantation. However, it is important to understand the material–host interactions that occur with implant debris to determine the aetiology of inflammation and tissue destruction around the prostheses. Owing to the limitations of *in vitro* models, and the limited access to, and scope, for intervention in human joint tissue, an *in vivo* model

*Author for correspondence (m.h.grant@strath.ac.uk).

Electronic supplementary material is available at http://dx.doi.org/10.1098/rsif.2012.0006 or via http://rsif.royalsocietypublishing.org.

Received 4 January 2012
Accepted 20 March 2012

of host interactions with MoM particles would provide the most useful information. There have been a number of animal prosthetic implant models reported; however, many of these are extremely complex, time-consuming and expensive. The rodent air-pouch model, originally described by Sedgwick and co-workers [7], was developed as a facsimile synovium for the study of inflammatory processes. It is a more straightforward approach than prosthetic implants and allows the quantification and analysis of cellular infiltration and mediators within the pouch cavity and surrounding tissue in response to implanted materials. The model has previously been used to assess the inflammatory responses to orthopaedic materials [8,9].

The aim of this study was to investigate the acute inflammatory responses to wear debris from MoM hip prostheses within the rodent air-pouch model using tissue histology, flow cytometric analysis of leukocyte infiltrates and multiplex polymerase chain reaction (PCR). This comprehensive approach has allowed a more complete understanding of the basic processes induced by cobalt–chromium (CoCr) wear debris that may contribute to ARMD and ultimately joint failure.

2. METHODS

2.1. Preparation of wear debris

CoCr wear debris was donated by DePuy International (Leeds, UK). A high-carbon cast cobalt chrome hip resurfacing implant was worn on a multi-station hip joint simulator using a non-standard protocol. The wear debris was produced over 2 50 000 cycles using distilled water as the lubricating fluid. Production of the debris in water obviated the need for complex debris extraction techniques to remove the serum prior to implanting the debris into mice. The use of only distilled water (instead of the more usual bovine serum (25%) in distilled water) resulted in a more aggressive wear regime which produced a greater volume of wear debris of similar morphology and size to that produced under similar conditions in 25 per cent serum (Dr C. Hardaker 2011, DePuy International, personal communication). The wear debris produced by the hip simulator under several different conditions has previously been shown to be of similar size and morphology [10].

Once produced, the wear debris, which was suspended in distilled water, was centrifuged at 3500*g* for 20 minutes. The majority of the water was then aspirated. The remaining suspension was heat-treated (180°C for 5 h, 60 kPa) in a vacuum oven to eliminate the remaining water and destroy any endotoxin. The dry debris was then suspended in sterile phosphate-buffered saline (PBS; Invitrogen; Paisley, UK).

The sterility of the treated wear debris was tested by exposing dendritic cells (isolated from bone marrow of male BALB/c (Harlan, UK) mouse femurs and tibias [11]) to the debris for 24 h, *in vitro*, and then assessing the expression of surface activation markers via flow cytometry. The debris was found not to increase the surface expression of CD40, CD86 or MHC II on these cells, and, therefore, the suspended debris was deemed sterile and endotoxin-free (data not shown).

2.2. Characterization of wear debris

The wear debris was imaged using a Hitachi TM-1000 scanning electron microscope (SEM). Samples were examined at magnifications of 800–7000× and digital images obtained. Energy dispersive X-ray spectroscopy (EDS) was used for quantitative analysis of the elemental composition. Hitachi TM-1000 and EDSwift-TM software was used to obtain the images and chemical spectra of the wear debris.

2.3. Exposure to wear debris

Air-pouches were generated according to a modified method of that described by Sedgewick *et al.* [7]. An area of the lower dorsal skin of an eight to 10-week-old male, BALB/c mouse was cleaned with alcohol and shaved. A subcutaneous injection of 1 ml of sterile air was injected at a single site in this area with a 25 gauge needle and 1 ml syringe (both BD Bioscience; Oxford, UK). Three days later, air-pouches were injected with 0.5 ml of sterile air to maintain the pouch.

Three days following the second injection, the pouches were injected with either 2.5 mg of sterile wear debris or 1 µg lipopolysaccharide (LPS; from *Salmonella abortus equi*; Sigma-Alrich, Dorset, UK) each of which was dissolved in 500 µl of sterile PBS. Negative control animals were injected with 500 µl of sterile PBS alone. A 23.5 gauge needle (BD Bioscience; Oxford, UK) was used to carry out these injections. In order to avoid pain the mice were briefly anaesthetized with isoflurane for the earlier procedures.

2.4. Inflammatory exudate

The inflammatory exudates were recovered from the air-pouches at 4, 24, 48 and 72 h post implantation. To achieve this, the pouches were lavaged with 500 µl of sterile PBS using a 21 gauge needle (BD Bioscience; Oxford, UK).

2.5. Flow cytometry analysis of inflammatory exudate

The cells were counted on a haemocytometer using Trypan Blue (Sigma-Aldrich; Dorset, UK) exclusion to assess viability. They were then stained with lineage specific monoclonal antibodies to distinguish neutrophils, monocytes/macrophages and B and T lymphocytes. Neutrophils were $Ly6G^+$ (clone RB6-8C5), monocytes/macrophages were $CD11b^+$ (clone M1/70), B-lymphocytes were $B220^+$ (clone RA3-6B2) and T-lymphocytes were $CD3^+$ (clone 500A2) (all eBioscience; Hatfield, UK). Briefly, cells were suspended in 100 µl FACS (fluorescence-activated cell sorting) buffer (PBS, 2% (v/v) foetal calf serum, and 0.05% (w/v) NaN_3) containing Fc Block (2.4G2 hybridoma supernatant) and the appropriate combinations of antibodies. After washing with FACS buffer, samples were analysed using a FACSCanto flow cytometer (BD Bioscience; Oxford, UK) and data assessed using FlowJo software (Tree Star, Ashland, OR, USA).

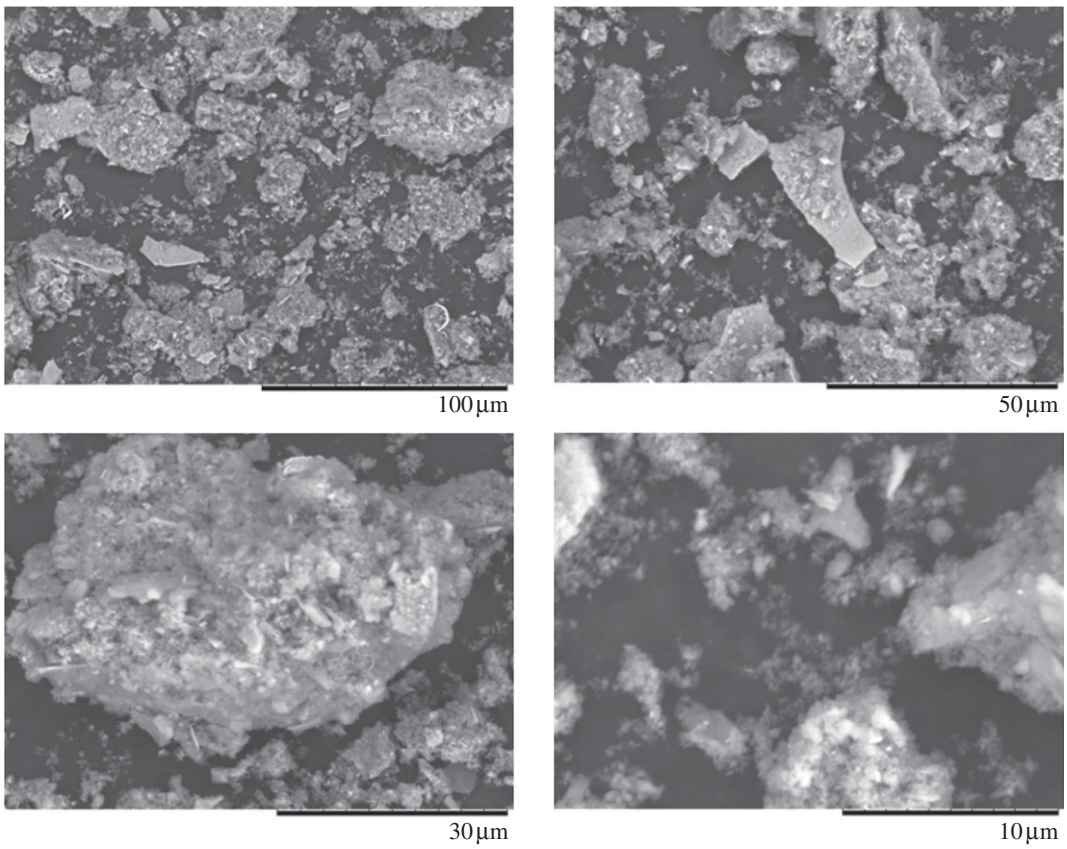

Figure 1. Scanning electron microscopy images of wear debris from a hip resurfacing implant. Image taken at 800–7000×.

2.6. Histological evaluation of air-pouch

The pouches were dissected at 4, 24, 48 and 72 h and 7 days post implantation. These were fixed in 10 per cent formalin (Sigma-Aldrich; Dorset, UK) for histological evaluation. These samples were sectioned and stained with haematoxylin and eosin (H&E) by Veterinary Diagnostic Services, University of Glasgow (Glasgow, UK). The samples were mounted onto glass microscope slides, and viewed under a Carl Zeiss Axio Imager microscope using a 10–40× air lens. Digital images were captured and analysed using AxioVision v. 4.6. Pouch membrane thickness was determined at six points on each section, with an even distribution of measurement. The total number of cells (based upon nucleus count) was determined as cells per square millimetre.

2.7. TaqMan low density array analysis

TaqMan low density arrays (TLDA) are 384-well microfluidic cards that can perform 384 real-time PCR reactions simultaneously. The card allows several samples to be run in parallel against a range of gene targets that are pre-loaded into each of the wells on the card. A custom plate was designed with a 32-gene format, allowing the analysis of four different isolates per plate, each tested for 32 different target genes in triplicate.

The plates contained primer pairs for a wide range of chemokines and cytokines plus a mandatory internal control against 18S ribosomal gene and a second TATA-binding protein control. The complete list of gene targets and primer sequences is included in electronic supplementary material, figure S1.

Tissues from the air-pouches treated with PBS, LPS or CoCr debris were excised, macerated and transferred to RLT lysis buffer (Qiagen; Crawley, UK) containing 0.1 per cent mercaptoethanol. The tissue was then homogenized by sonication on ice, and mRNA isolated from each sample using a Qiagen RNEasy kit as per manufacturer's instructions. The mRNA was quantified using a Nanodrop 1000 (Thermo Scientific; Hertfordshire, UK), normalized and converted to cDNA using an AffinityScript kit (Applied Biosystems; Warrington, UK), including a DNase step. The cDNA was loaded onto the TLDA plates at 1 µg per lane after 1 : 1 dilution with TaqMan PCR Mastermix (no AMPErase; Applied Biosystems) and run on a 7900HT TaqMan reader using standard SDS software. ΔCt values were generated by normalizing to 18S for each treatment and ΔΔCt values by normalizing to the mean ΔCt from the PBS-treated air-pouch control. The relative quantitation value was then calculated as $2^{-\Delta\Delta Ct}$.

Results were expressed as fold change over the untreated control. Data are shown as means plus standard error of the mean from three independent experiments.

3. RESULTS

3.1. Characterization of cobalt–chromium wear debris

The wear debris produced on a hip simulator from the ASR hip resurfacing implant are shown in figure 1.

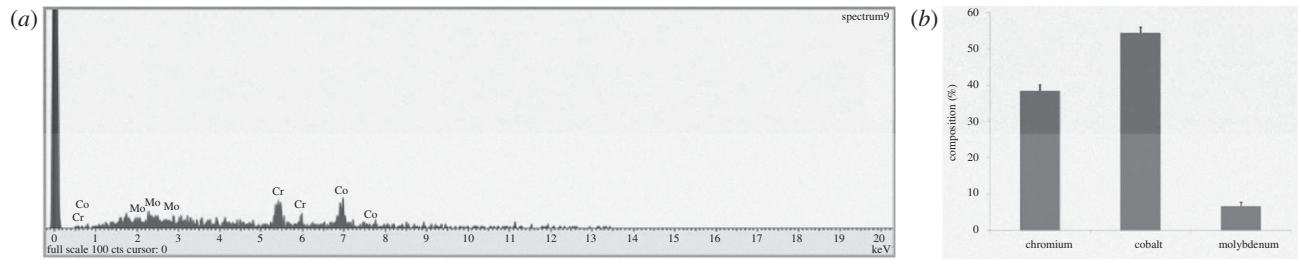

Figure 2. Energy dispersive X-ray spectroscopy of wear debris from a hip resurfacing implant. (*a*) Spectroscopic data of wear debris. (*b*) Composition of CoCr wear debris from hip resurfacing implant. Results are means ± s.e.m., $n = 25$.

The SEM images indicate a wide variety of irregular shaped particles. The debris varies in size, from micrometer to nanometre. The larger irregular particles appear to be aggregates of smaller particles. EDS indicated that the wear debris is primarily composed of cobalt (figure 2). Analysis of 25 different particles indicated a mean composition of 54.48 per cent cobalt and 38.43 per cent chromium, with a small percentage of molybdenum being present.

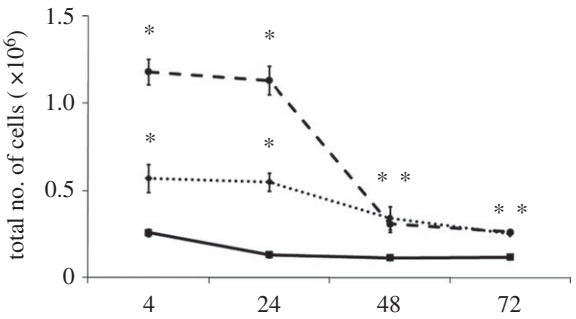

Figure 3. Total number of cells present in the inflammatory exudates at different time points. Cells were collected from the air-pouches following the injection of PBS (solid line with squares), CoCr (dotted line with diamonds) debris or LPS (dashed line with circles). Results are means ± s.e.m. ($n = 3$). Asterisks (*) denote significantly different from PBS (negative control) values ($p < 0.05$) by one-way ANOVA followed by Dunnett's multiple comparison test.

3.2. Inflammatory exudate

The cellular kinetics of the acute inflammatory response to CoCr wear debris are shown in figures 3–5. The air-pouches were injected with either sterile PBS, CoCr debris or, LPS as a positive control [12]. The data in figure 3 show only a low level of cellular infiltrate in air-pouches injected with PBS. Both CoCr debris and LPS caused a significant increase in the number of cells recovered from the inflammatory cavity at all time points. The highest numbers of cells recovered were at 4 h post implantation, with means of 5.7×10^5 and 11.8×10^5 cells from the CoCr debris and LPS-treated mice, respectively.

Cells within the inflammatory exudate were identified by flow cytometry following surface antigen staining (figure 4). Neutrophils were $Ly6G^+$ and $CD11b^+$, monocytes/macrophages were $CD11b^+$, B-lymphocytes were $B220^+$ and T-lymphocytes were $CD3^+$. An example of this is shown in figure 4*a*. The data indicate that LPS caused a significant increase in neutrophil infiltration at 4 and 24 h compared with PBS control values (figure 4*b*). Although there were higher levels of neutrophils within the inflammatory exudate of CoCr debris exposed animals compared with PBS exposed, this increase was not significant ($p > 0.05$). Both CoCr debris and LPS induced a significant increase in the number of monocyte/macrophage within the pouch cavity 4 and 24 h post-injection. There was also a higher level of these cells present in the inflammatory exudate recovered from LPS-treated mice at 72 h.

In contrast to neutrophils and monocytes/macrophages, both T and B-lymphocytes were present in low numbers. An elevation in T-lymphocytes was observed only 48 h after CoCr debris implantation. Both LPS and CoCr debris induced a small but significant increase in the number of B-lymphocytes present in the inflammatory exudate at 72 h, compared with PBS treatment. The pouches at 7 days appeared to have collapsed and hence could not be lavaged accurately.

3.3. TaqMan low density arrays analysis of inflammatory factor expression in air-pouches

Air-pouch tissue taken at 24 h post-injection of LPS, CoCr debris or PBS was assessed for the presence of transcripts encoding a panel of pro- and anti-inflammatory cytokines and chemokines as outlined in electronic supplementary material, figure S1. The data were calculated as fold change over the PBS control air-pouch levels and are shown in figure 5. Many of the target cytokines or chemokines were not detected in the air-pouch tissue (e.g. IFN-γ, IL-4 or CCL19), or showed no discernible change from the PBS control tissue (CXCL12, TATA-binding protein). However, in both LPS and CoCr debris-treated tissue there were major increases in the inflammatory cytokine, IL-1β, and the chemokines; CCL2 and CXCL2, with LPS treatment causing the greatest fold change over the PBS control. The chemokine transcript levels correlate well with inflammatory exudates, as CXCL2 is a potent chemotactic factor for neutrophil recruitment, whereas CCL2 is a key factor inducing macrophage migration. There was evidence that LPS and CoCr induced a different pattern of inflammatory response, with LPS causing strong increases in

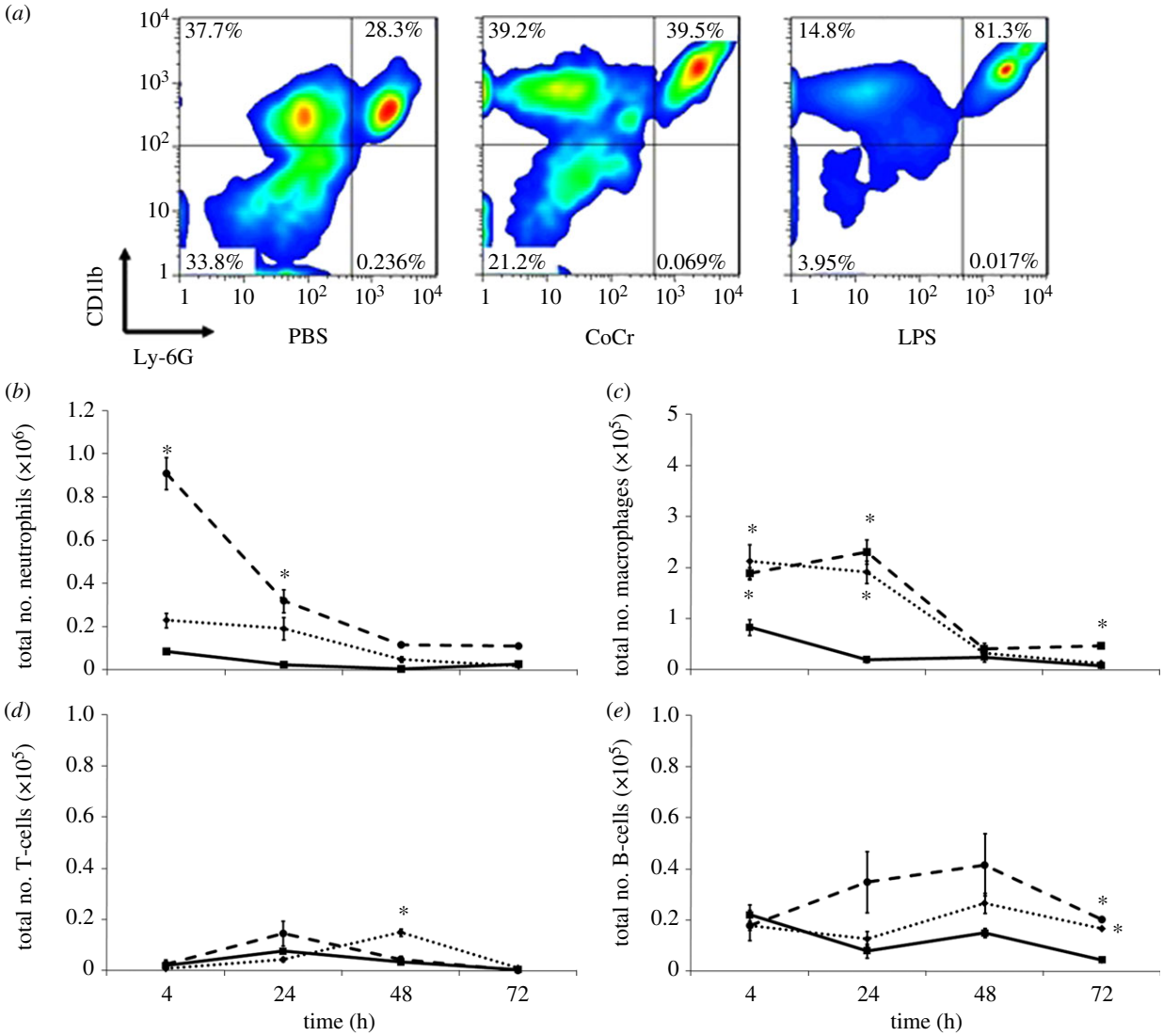

Figure 4. A flow cytometric analysis of the inflammatory exudate recovered at different time points. (*a*) Identification of cells within the inflammatory exudate recovered 4 h post implantation; cells that were Ly-6G$^+$ and CD11b$^+$ were determined to be neutrophils, Ly-6G$^-$ and CD11b$^+$ cells were identified as monocytes/macrophages. (*b*) Number of neutrophils, (*c*) monocytes/macrophages, (*d*) T-lymphocytes and (*e*) B-lymphocytes present in the inflammatory exudates at different time points following injection of PBS (solid line with squares), CoCr (dotted line with diamonds) debris or LPS (dashed line with circles). Results are means $\pm$ s.e.m. ($n = 3$). Asterisks (*) denote significantly different from PBS (negative control) values ($p < 0.05$) by one-way ANOVA followed by Dunnett's multiple comparison test. (Online version in colour.)

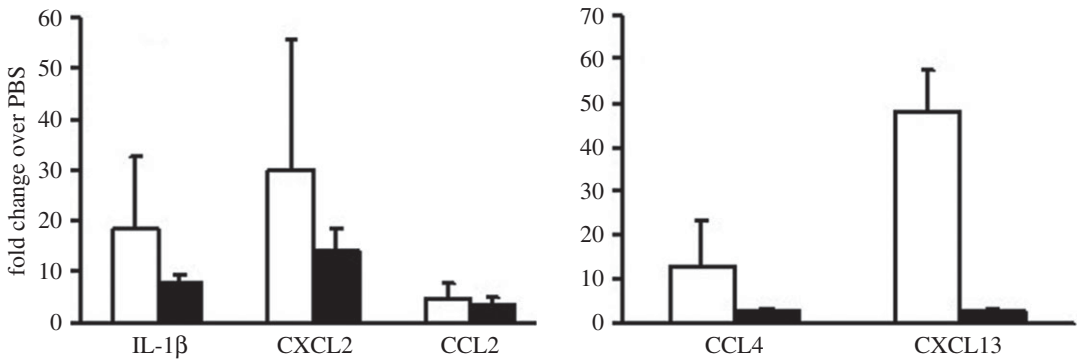

Figure 5. Inflammatory factor transcripts in air-pouch tissue at 24 h post-injection. The mRNA from air-pouch tissue from mice treated with LPS (open bars) or CoCr (filled bars) debris was assessed using TLDA analysis, and expressed as fold change over levels from PBS-injected air-pouch. Results are shown as means $\pm$ s.e.m. ($n = 3$). No significant difference ($p > 0.05$) was measured when compared with PBS values by one-way ANOVA followed by Dunnett's multiple comparison test.

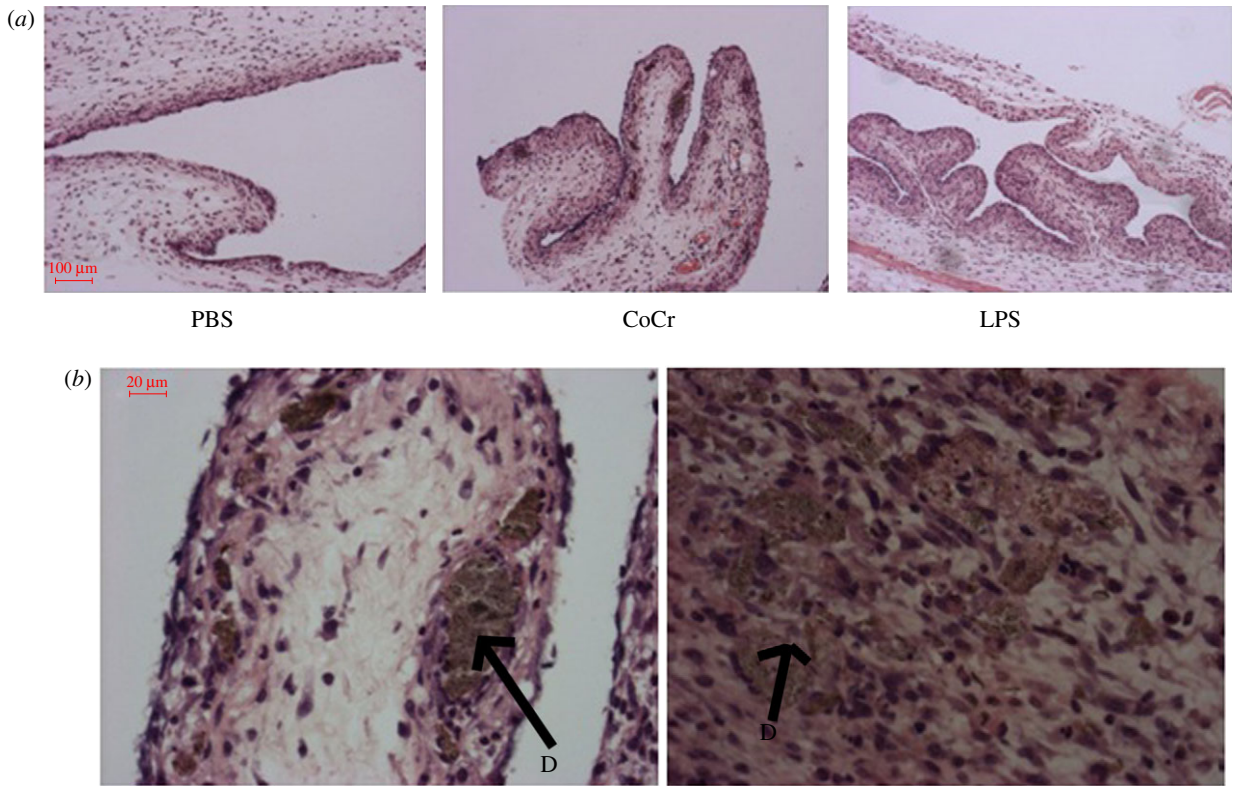

Figure 6. The histological appearance of negative (PBS) and positive (LPS) control and CoCr-treated air-pouch membranes, 24 h post-injection. (*a*) Images taken at 10× magnification of PBS-, CoCr- and LPS-treated air-pouch membranes. (*b*) Images taken at 40× magnification of CoCr-treated air-pouch membranes. 'D' indicates CoCr debris within the tissue. (Online version in colour.)

CCL4 and CXCL13 which was not mirrored by CoCr stimulation. Owing to the small sample number and variation in tissue response between individuals, the data did not show clear significance ($p \geq 0.06$).

3.4. Histological evaluation and image analysis

The histological appearance of the air-pouches 24 h following treatment is displayed in figure 6. All the pouches are typically characterized by an outer fibrous layer and an inner layer mainly consisting of inflammatory cells. Consistent with the flow cytometry analysis of exudate cells, at 24 h the LPS-treated pouches appear more inflamed, with increased cellularity compared with PBS-treated pouches. Interestingly, at 24 h CoCr debris appears to have migrated into the pouch tissue and was surrounded by inflammatory cells (figure 6); these cells appear to be surrounding the CoCr wear debris in an organized manner.

At 72 h, the CoCr debris-treated pouches show that the debris, marked D, is embedded in the inner layer of the pouch (figure 7). Further examination shows some cell death and a wide area of necrotic tissue around the embedded CoCr debris (area marked A in figure 7*b*). There also appears to be the formation of fibrous tissue around the debris as shown by the area marked F in figure 7*b*.

At 7 days post-injection, PBS- and LPS-treated pouches appear to have collapsed (figure 8*a*). The inflammatory layer can be identified, but is less pronounced than at earlier time points. However, a large cellular infiltrate is apparent within the CoCr debris-treated air-pouches, with the majority of cells having histological characteristics of monocytes. Figure 8 indicates that these cellular infiltrates are concentrated in areas where CoCr debris is present. There are a number of areas (marked A on figure 8*b*) where there appears to be cellular debris in the CoCr debris-treated pouches. This figure also displays the encapsulation of the wear debris within fibrous tissue (F on figure 8*b*) and a spherical mass of inflammatory cells surrounding the debris, similar to granuloma histology.

The results of histological parameters (membrane thickness and cellularity) were measured from images taken from all samples (figure 9). Although both LPS- and CoCr-treated pouches had thicker membranes than PBS-treated pouches, this was not found to be significant (figure 9*a*).

Figure 9*b* indicates that both CoCr and LPS have a significantly higher cellularity within the air-pouch at 24 and 72 h post-injection, compared with PBS values. The highest density of cells infiltrating the pouch membrane was observed at 72 h for all the air-pouches. The cellularity at this time point was 3614 ± 418, 4730 ± 372 and 7048 ± 1162 cells mm^{-2} in PBS-, CoCr- and LPS-treated pouches, respectively. These data also indicate that CoCr pouches have a significantly higher cellularity than PBS-treated pouches 7 days post implantation, whereas LPS did not.

4. DISCUSSION

The current study has described the acute inflammatory effects of CoCr wear debris from a hip

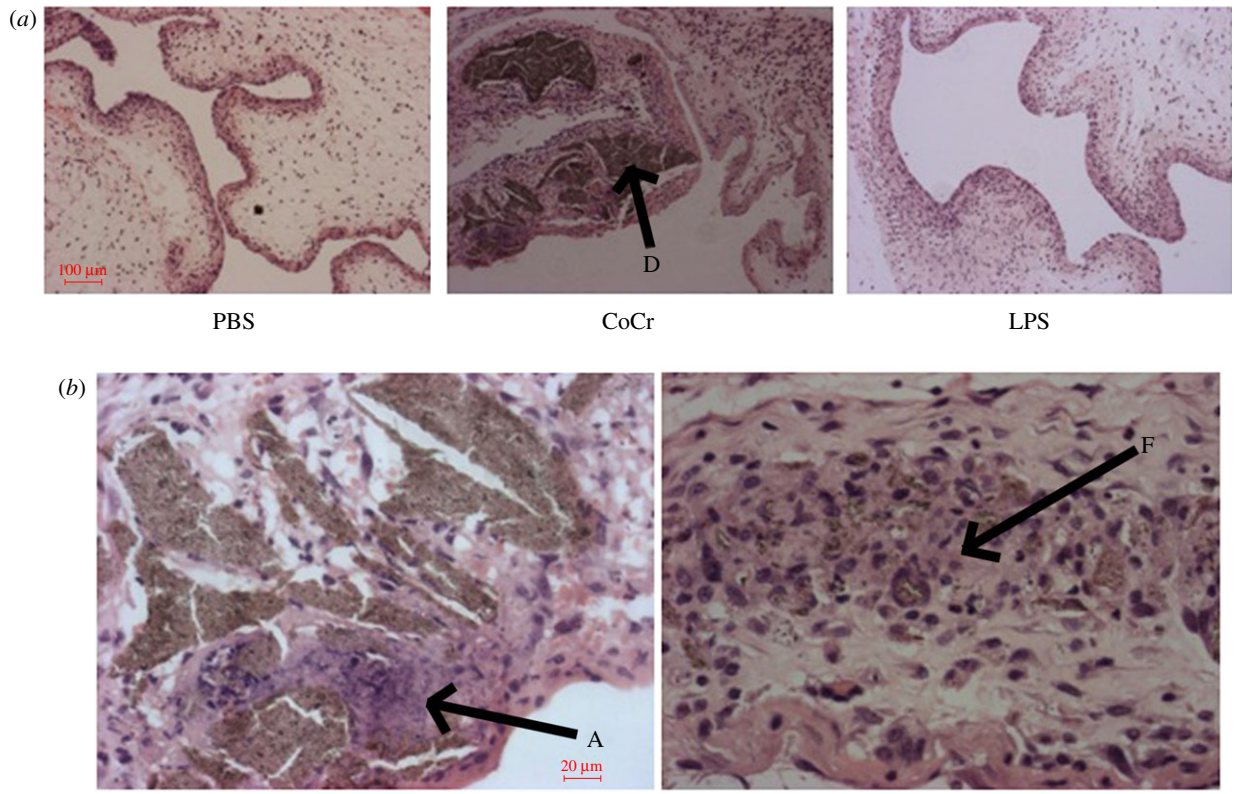

Figure 7. The histological appearance of negative (PBS) and positive (LPS) control and CoCr-treated air-pouch membranes, 72 h post-injection. (*a*) Images taken at 10× magnification of PBS-, CoCr- and LPS-treated air-pouch membranes. 'D' indicates CoCr debris within the tissue. (*b*) Images taken at 40× magnification of CoCr-treated air-pouch membranes. 'A' indicates areas of cell death, 'F' indicates fibrotic tissue. (Online version in colour.)

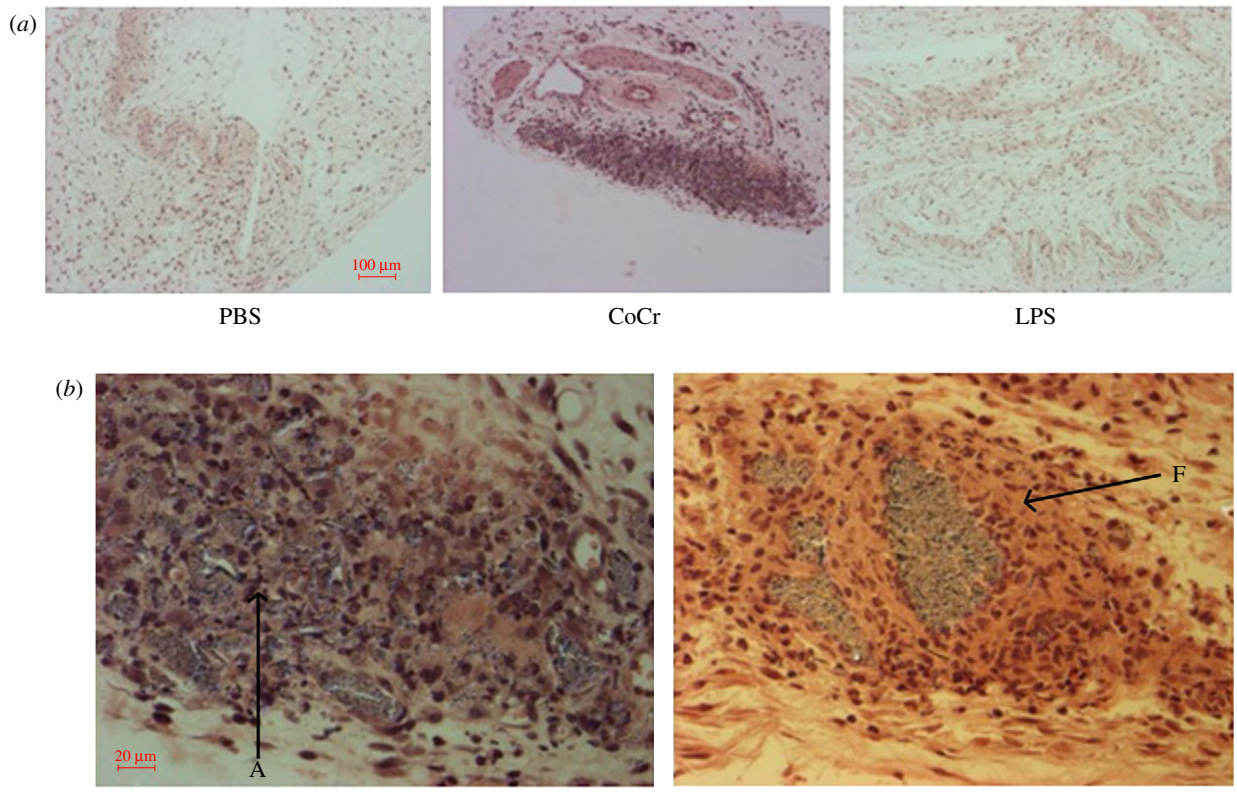

Figure 8. The histological appearance of negative (PBS) and positive (LPS) control and CoCr-treated air-pouch membranes, 7 days post-injection. (*a*) Images taken at 10× magnification of PBS-, CoCr- and LPS-treated air-pouch membranes. (*b*) Images taken at 40× magnification of CoCr-treated air-pouch membranes. 'A' indicates areas of cell death, 'F' indicates fibrotic tissue. (Online version in colour.)

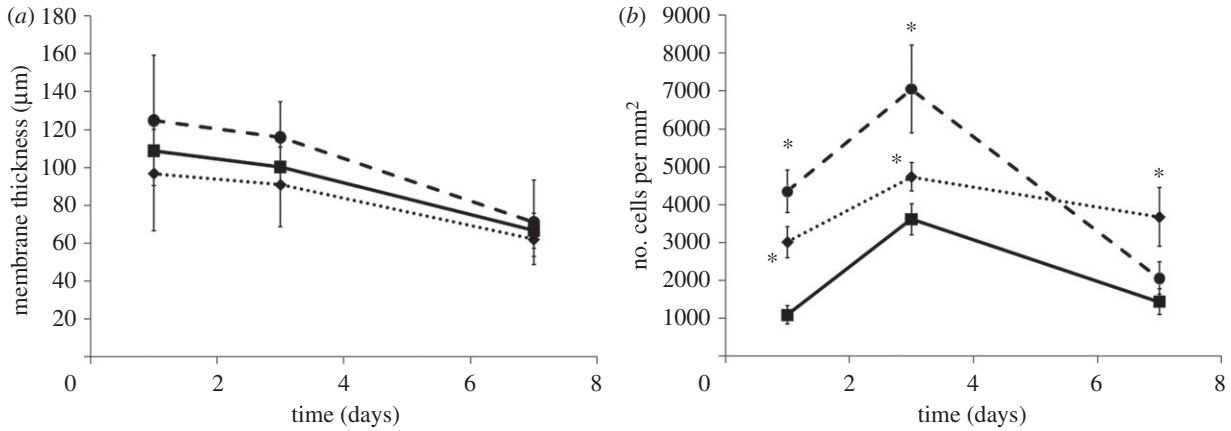

Figure 9. (*a*) Membrane thickness of air-pouch tissue and (*b*) number of cells in air-pouch tissue following treatment with PBS (solid line with squares), CoCr (dotted line with diamonds) debris or LPS (dashed line with circles). Results are means ± s.e.m. ($n = 3$). Asterisks (*) denote significantly different from PBS (negative control) values ($p < 0.05$) by one-way ANOVA followed by Dunnett's multiple comparison test.

resurfacing prosthesis. CoCr wear debris, from a hip resurfacing implant, was found to range in size and shape. These irregularly shaped particles ranged from the nanometre scale to micrometre particles; some of the latter were aggregates of the smaller particles. Owing to the irregular nature of these particles it was difficult to accurately quantify their number or measure their surface area. Therefore, the dose for implantation studies was quantified as a dry mass that could easily be suspended in PBS and implanted via a simple injection. Previous simulator testing has shown that around 8 mm^3 of debris per million cycles was produced under harsh conditions [13,14]. The density of the CoCr alloy used to produce the wear debris was approximately 8.32 $mg\,mm^{-3}$, as a result, 8 mm^3 of wear would equate to 66.6 mg of debris [15]. Therefore, the authors concede that 2.5 mg per approximately 20 g mouse could be a relatively high dose compared with 66.6 mg per approximately 75 kg patient.

These sterile CoCr wear debris particles were injected into a rodent air-pouch allowing the investigation of local inflammatory processes that may be induced following the release of particles from MoM hip arthroplasty. Flow cytometry revealed that CoCr debris induced significant recruitment of inflammatory cells into the pouch cavity; primarily neutrophils and macrophages/monocytes at 24–48 h post-injection. However, the CoCr debris appeared to induce quite a different inflammatory pattern compared with the positive control (LPS) in terms of cellular composition and chemokine profile. As expected, LPS-induced inflammation was characterized by initially high numbers of neutrophils, followed by increased levels of monocyte/macrophages [12]. In contrast, CoCr debris induced a different cellular different response to LPS containing similar numbers of neutrophils and monocyte/macrophage within the pouch cavity. Thus, CoCr debris induced lower levels of neutrophil infiltrate compared with LPS but had similar levels of monocyte/macrophage infiltrate within the pouch cavity. This correlates well with the inflammatory factor transcript data from the air-pouch tissue, which indicated that LPS stimulation resulted in a mean 30-fold up-regulation of the neutrophil-recruiting chemokine CXCL2 [16]. In contrast, CoCr stimulation resulted in only an 18-fold increase. Both LPS and CoCr showed a similar three to fourfold increase in CCL2, a potent monocyte and macrophage migration factor [17], which resulted in similar absolute numbers of macrophages in the tissue and exudate. During the early phase of CoCr debris-induced inflammation, neither T nor B-lymphocytes seemed to be significantly attracted to the air-pouch cavity, although there was an increase in B-lymphocytes at 72 h. The cellular phenotype present in inflammatory responses generally varies with time from induction with phagocytes being predominant during the early phases of inflammation, whereas lymphocytes become more evident in chronic inflammation [18]. It was not possible to lavage the air-pouch after 72 h and the point at which lymphocyte migration into the cavity occurred could therefore not be determined.

The histological data further demonstrate that CoCr debris provokes a specific acute inflammatory response with an appearance distinct from that induced by LPS. LPS stimulation led to pronounced upregulation of certain chemokines such as CCL4 and CXCL13, which were not induced by CoCr stimulation. Additionally, CoCr wear debris led to the development of large inflammatory infiltrates in the air-pouch tissue. The majority of these cells were localized around the debris that became embedded deep within the tissue. The cells surrounding this debris appeared to be mainly monocytes/macrophages, and even with this acute exposure the pattern in the current *in vivo* model strongly resembled peri-prosthetic tissue recovered from revision surgery [19]. There was also granuloma formation and increased levels of fibrous tissue around the debris, especially at later time points. There was some evidence even at 24 h that CoCr debris caused an increase in TGF-β gene expression (2.26-fold increase over both PBS and LPS stimulation), which has a role in wound resolution, scarring and fibrosis. Again this is reminiscent of previous histological findings that have been described in ARMD [20,21]. Previous histological data have also shown that tissue necrosis around the prosthesis is a hallmark of ARMD and joint failure [5,21], and the findings of the present study support this.

Although LPS also induces inflammatory processes such as cellular infiltrates, this appears to be spread over the whole area of the pouch, whereas the response to CoCr appears to be localized around the debris. This is particularly evident at the longer time points post implantation. While the number of cells within the tissue of LPS-treated pouches is reduced at 7 days, the level of cellular infiltration in the CoCr debris-treated pouches remains constant. Although the current study has only examined exudate and tissue response at an acute phase, the presence of mononuclear cells (primarily monocytes and macrophages) and the non-uniform histological appearance of the pouch tissue are indicative of a chronic inflammatory response to this biomaterial [22]. This further indicates that CoCr debris initiates a chronic, monocyte/macrophage mediated process within the current model.

The current study has shown that sterile CoCr debris initiates a distinct acute inflammatory process which can lead to a high level of monocyte/macrophage infiltration. It has previously been shown that *in vitro* exposures of monocytes and macrophages to CoCr wear debris resulted in an upregulation of antigen presentation and pro-inflammatory properties of these cells [23,24]. These *in vitro* studies have shown that CoCr wear debris leads to increased expression of co-stimulatory surface molecules as well as increased macrophage reactivity. In particular, these studies have demonstrated an increase in secretion of the pro-inflammatory cytokine IL-1β, in the response to CoCr wear debris, which was confirmed by transcript data from the present study. These *in vitro* results also correlate with *in vivo* responses observed following implantation of CoCr engineered particles [8]. The increasing evidence implying a central role for IL-1β in metal-induced pro-inflammatory effects has led to the suggestion that IL-1 receptor antagonists may be used as a therapeutic intervention for implant debris induced inflammation [23].

In addition, several studies have shown that metal ions from orthopaedic implants can directly affect inflammatory cells [25,26]. It is widely reported that metal ions are released from MoM hip implants, whether directly or via wear debris formation [27–29]. These ions, particularly chromium and cobalt, have been shown to be elevated locally around the joint and systemically in blood following MoM hip resurfacing arthroplasty [30]. Caicedo *et al.* [24] describe a biphasic response in monocytes exposed to metal ions *in vitro*. Lower levels of these ions were found to be stimulatory, whereas higher levels have a toxic effect on monocytes. High levels of chromium and cobalt ion exposure *in vitro*, are known to induce cell death in a number of immune system cells such as lymphocytes, monocytes and macrophages [31–33]. It is possible that the cell death observed around the CoCr debris in the pouches was induced by ions released from the CoCr wear debris. In addition, the surface chemistry of the wear debris may facilitate cell death following cellular adhesion [34]. However, cell death in the form of apoptosis is also the natural end process of inflammation and wound healing [35]. Therefore, the cell death observed in the current model may also be part of the acute inflammatory response associated with CoCr debris.

The histological data indicate that the implanted CoCr debris becomes encapsulated by fibrous tissue and inflammatory cells by day 7. Biomaterial implantation has previously been shown to induce fibrosis or fibrous capsule development [36]. This process has been observed in patients following MoM hip resurfacing surgery and, in particular, has been defined as the major histological feature from soft tissue around loose implants [37]. High levels of macrophages/monocytes around the debris may facilitate this process because activated macrophages are reported to produce pro-fibrotic factors, which enhance fibrogenesis by fibroblasts [38]. This fibrotic response, as well as the above-mentioned cell infiltrates and cell death, was only observed in the CoCr-treated air-pouches. Because these are not observed in the inflammatory response to LPS, it is a fair assumption that this is a processes induced by CoCr wear debris.

It is clear that the current acute *in vivo* model produces a number of features resembling processes identified in the pathology of ARMD. The release of wear debris *in situ* is continuous for the duration of the implant, whereas the current model only provides the equivalent of a single release of wear debris leading to a transient response. Repeated doses of CoCr debris should be administered in future studies for complete evaluation of the chronic responses induced following MoM arthroplasty. In addition, this model could be used to assess the specific effects induced by wear debris of novel material bearing couples.

5. CONCLUSION

Implantation of CoCr wear debris from a MoM hip resurfacing implant induces an inflammatory process that is different from that induced by LPS. The process involves infiltration of inflammatory cells, primarily monocytes/macrophages, as well as granuloma and fibrous capsule formation and tissue necrosis around the debris. Monocytes/macrophages not only have a key role in the earlier-mentioned processes in the *in vivo* mouse model but may also be highly significant in the chronic inflammatory response observed with ARMD in patients.

M.A. is the recipient of a Case Award PhD Studentship from the EPSRC and DePuy International Ltd. Aspects of the study were supported by a programme grant from Medical Research Council awarded to G.J.G.

REFERENCES

1 National Joint Registry. 2010 Seventh Annual Report: National Joint Registry for England and Wales. See http://www.njrcentre.org.uk.
2 Macpherson, G. & Breusch, S. 2010 Metal-on-metal hip resurfacing: a critical review. *Arch. Orthop. Trauma Surg.* **131**, 101–110. (doi:10.1007/s00402-010-1153-9)
3 Ingham, E. & Fisher, J. 2000 Biological reactions to wear debris in total joint replacement. *Proc. Inst. Mech. Eng. H* **214**, 21–37. (doi:10.1243/0954411001535219)
4 Counsell, A., Heasley, R., Arumilli, B. & Paul, A. 2008 A groin mass caused by metal particle debris after hip resurfacing. *Acta Orthop. Belg.* **74**, 870–874.

5 Willert, H.-G., Buchhorn, G. H., Fayyazi, A., Flury, R., Windler, M., Koster, G. & Lohmann, C. H. 2005 Metal-on-metal bearings and hypersensitivity in patients with artificial hip joints. A clinical and histomorphological study. *J. Bone Joint Surg.* **87**, 28–36. (doi:10.2106/JBJS.A.02039pp)

6 Hallab, N., Caicedo, M., Finnegan, A. & Jacobs, J. 2008 Th1 type lymphocyte reactivity to metals in patients with total hip arthroplasty. *J. Orthop. Surg. Res.* **3**, 6. (doi:10.1186/1749-799X-3-6)

7 Sedgwick, A. D., Sin, Y. M., Edwards, J. C. W. & Willoughby, D. A. 1983 Increased inflammatory reactivity in newly formed lining tissue. *J. Pathol.* **141**, 483–495. (doi:10.1002/path.1711410406)

8 Wooley, P. H., Morren, R., Andary, J., Sud, S., Yang, S.-Y., Mayton, L., Markel, D., Sieving, A. & Nasser, S. 2002 Inflammatory responses to orthopaedic biomaterials in the murine air pouch. *Biomaterials* **23**, 517–526. (doi:10.1016/S0142-9612(01)00134-X)

9 Barbosa, J. N., Barbosa, M. A. & Águas, A. P. 2004 Inflammatory responses and cell adhesion to self-assembled monolayers of alkanethiolates on gold. *Biomaterials* **25**, 2557–2563. (doi:10.1016/j.biomaterials.2003.09.047)

10 Brown, C., Williams, S., Tipper, J., Fisher, J. & Ingham, E. 2007 Characterisation of wear particles produced by metal on metal and ceramic on metal hip prostheses under standard and microseparation simulation. *J. Mater. Sci. Mater. Med.* **18**, 819–827. (doi:10.1007/s10856-006-0015-z 123)

11 Lutz, M. B., Kukutsch, N., Ogilvie, A. L. J., Rößner, S., Koch, F., Romani, N. & Schule, G. 1999 An advanced culture method for generating large quantities of highly pure dendritic cells from mouse bone marrow. *J. Immunol. Methods* **223**, 77–92. (doi:10.1016/S0022-1759(98)00204-X)

12 Kadl, A., Galkina, E. & Leitinger, N. 2009 Induction of CCR2-dependent macrophage accumulation by oxidized phospholipids in the air-pouch model of inflammation. *Arthritis Rheum.* **60**, 1362–1371. (doi:10.1002/art.24448)

13 Leslie, I., Williams, S., Brown, C., Isaac, G., Jin, Z., Ingham, E. & Fisher, J. 2008 Effect of bearing size on the long-term wear, wear debris, and ion levels of large diameter metal-on-metal hip replacements—an *in vitro* study. *J. Biomed. Mater. Res. B* **87B**, 163–172. (doi:10.1002/jbm.b.31087)

14 Williams, S., Leslie, I., Isaac, G., Jin, Z., Ingham, E. & Fisher, J. 2008 Tribology and wear of metal-on-metal hip prostheses: influence of cup angle and head position. *J. Bone Joint Surg.* **90**(Suppl. 3), 111–117. (doi:10.2106/jbjs.h.00485)

15 Medley, J. B., Chan, F. W., Krygier, J. J. & Bobyn, J. D. 1996 Comparison of alloys and designs in a hip simulator study of metal on metal implants. *Clin. Orthop. Relat. Res.* **329**(Suppl.), 148–159. (doi:10.1097/00003086-199608001-00015)

16 Wolpe, S. D., Sherry, B., Juers, D., Davatelis, G., Yurt, R. W. & Cerami, A. 1989 Identification and characterization of macrophage inflammatory protein 2. *Proc. Natl Acad. Sci. USA* **86**, 612–616. (doi:10.1073/pnas.86.2.612)

17 Deshmane, S. L., Kremlev, S., Amini, S. & Sawaya, B. E. 2009 Monocyte chemoattractant protein-1 (MCP-1): an overview. *J. Interferon Cytokine Res.* **29**, 313–326. (doi:10.1089/jir.2008.0027)

18 Anderson, J. M. 1994 *In vivo* biocompatibility of implantable delivery systems and biomaterials. *Eur. J. Pharm. Biopharm.* **40**, 1–8.

19 Boss, J. H., Shajrawi, I., Soudry, M. & Mendes, D. G. 1990 Histological features of the interface membrane of failed isoelastic cementless prostheses. *Int. Orthop.* **14**, 399–403. (doi:10.1007/BF00182653)

20 Pandit, H. *et al.* 2008 Pseudotumours associated with metal-on-metal hip resurfacings. J. Bone Joint Surg. Br.**90-B**, 847–851. (doi:10.1302/0301-620X.90B7.20213)

21 Mahendra, G., Pandit, H., Kliskey, K., Murray, D., Gill, H. S. & Athanasou, N. 2009 Necrotic and inflammatory changes in metal-on-metal resurfacing hip arthroplasties. *Acta Orthop.* **80**, 653–659. (doi:10.3109/17453670903473016)

22 Anderson, J. M., Rodriguez, A. & Chang, D. T. 2008 Foreign body reaction to biomaterials. *Semin. Immunol.* **20**, 86–100. (doi:10.1016/j.smim.2007.11.004)

23 Caicedo, M. S., Desai, R., McAllister, K., Reddy, A., Jacobs, J. J. & Hallab, N. J. 2009 Soluble and particulate Co–Cr–Mo alloy implant metals activate the inflammasome danger signaling pathway in human macrophages: a novel mechanism for implant debris reactivity. *J. Orthop. Res.* **27**, 847–854. (doi:10.1002/jor.20826)

24 Caicedo, M. S., Pennekamp, P. H., McAllister, K., Jacobs, J. J. & Hallab, N. J. 2010 Soluble ions more than particulate cobalt-alloy implant debris induce monocyte costimulatory molecule expression and release of proinflammatory cytokines critical to metal-induced lymphocyte reactivity. *J. Biomed. Mater. Res. A* **93A**, 1312–1321. (doi:10.1002/jbm.a.32627)

25 Kwon, Y.-M., Xia, Z., Glyn-Jones, S., Beard, D., Gill, H. S. & Murray, D. W. 2009 Dose-dependent cytotoxicity of clinically relevant cobalt nanoparticles and ions on macrophages *in vitro*. *Biomed. Mater.* **4**, 025018. (doi:10.1088/1748-6041/4/2/025018)

26 Raghunathan, V. K., Tettey, J. N. A., Ellis, E. M. & Grant, M. H. 2009 Comparative chronic *in vitro* toxicity of hexavalent chromium to osteoblasts and monocytes. *J. Biomed. Mater. Res. A* **88A**, 543–550. (doi:10.1002/jbm.a.31893)

27 Schaffer, A. W., Schaffer, A., Pilger, A., Engelhardt, C., Zweymueller, K. & Ruediger, H. W. 1999 Increased blood cobalt and chromium after total hip replacement. *Clin. Toxicol.* **37**, 839–844. (doi:10.1081/CLT-100102463)

28 Vendittoli, P. A., Mottard, S., Roy, A. G., Dupont, C. & Lavigne, M. 2007 Chromium and cobalt ion release following the Durom high carbon content, forged metal-on-metal surface replacement of the hip. *J. Bone Joint Surg. Br.* **89-B**, 441–448. (doi:10.1302/0301-620X.89B4.18054)

29 Afolaranmi, G. A., Tettey, J., Meeh, R. M. D. & Grant, M. H. 2008 Release of chromium from orthopaedic arthroplasties. *Open Orthop. J.* **2**, 10–18. (doi:10.2174/1874325000802010010)

30 Langton, D. J., Sprowson, A. P., Joyce, T. J., Reed, M., Carluke, I., Partington, P. & Nargol, A. V. F. 2009 Blood metal ion concentrations after hip resurfacing arthroplasty: a comparative study of articular surface replacement and birmingham hip resurfacing arthroplasties. *J. Bone Joint Surg. Br.* **91-B**, 1287–1295. (doi:10.1302/0301-620X.91B10.22308)

31 Akbar, M., Brewer, J. M. & Grant, M. H. 2011 Effect of chromium and cobalt ions on primary human lymphocytes *in vitro*. *J. Immunotoxicol.* **8**, 140–149. (doi:10.3109/1547691X.2011.553845)

32 Vasant, C., Rajaram, R. & Ramasami, T. 2003 Apoptosis of lymphocytes induced by chromium(VI/V) is through ROS-mediated activation of Src-family kinases and caspase-3. *Free Radic. Biol. Med.* **35**, 1082–1100. (doi:10.1016/S0891-5849(03)00471-4)

33 Huk, O. L., Catelas, I., Mwale, F., Antoniou, J., Zukor, D. J. & Petit, A. 2004 Induction of apoptosis and necrosis by metal ions *in vitro*. *J. Arthroplasty* **19**(Suppl. 1), 84–87. (doi:10.1016/j.biomaterials.2004.11.019)

34 Brodbeck, W. G., Shive, M. S., Colton, E., Nakayama, Y., Matsuda, T. & Anderson, J. M. 2001 Influence of biomaterial surface chemistry on the apoptosis of adherent cells. *J. Biomed. Mater. Res.* **55**, 661–668. (doi:10.1002/1097-4636(20010615)55:4<661::AID-JBM1061>3.0.CO;2-F)

35 Greenhalgh, D. G. 1983 The role of apoptosis in wound healing. *Int. J. Biochem. Cell Biol.* **30**, 1019–1030. (doi:10.1016/S1357-2725(98)00058-2)

36 Gretzer, C., Emanuelsson, L., Liljensten, E. & Thomsen, P. 2006 The inflammatory cell influx and cytokines changes during transition from acute inflammation to fibrous repair around implanted materials. *J. Biomater. Sci. Polym. Ed.* **17**, 669–687. (doi:10.1163/156856206777346340)

37 McMinn, D., Treacy, R., Lin, K. & Pynsent, P. 1996 Metal on metal surface replacement of the hip: experience of the McMinn prosthesis. *Clin. Orthop. Relat. Res.* **329**(Suppl.), 89–98. (doi:10.1097/00003086-199608001-00009)

38 Song, E., Ouyang, N., Hörbelt, M., Antus, B., Wang, M. & Exton, M. S. 2004 Influence of alternatively and classically activated macrophages on fibrogenic activities of human fibroblasts. *Cell. Immunol.* **204**, 19–28. (doi:10.1006/cimm.2000.1687)